Gas in the central part of the nebula undergoes fast compression and forms a hot hydrostatic (not contracting) core containing a small fraction of the mass of the original nebula.
The gas of a circumstellar disk accretes onto the core.
The core gradually grows in mass until it becomes a young hot protostar.
At this stage, the protostar and its disk are obscured by the infalling envelope and are not directly observable.
Such objects are observed as very bright condensations, which emit mainly millimeter-wave and submillimeter-wave radiation - Class 0 protostars.

PROTOSTELLAR ENVELOPES: Class 0 source Barnard 1c in Perseus

- early protostellar collapse stage
- SEDs that resemble blackbodies with $T \leq 30$ K
- majority of the source mass resides in the infalling envelope
- exhibit powerful, bipolar molecular flows

PROTOSTELLAR ENVELOPES: Class 0 source Barnard 1c (B1-c) in Perseus

The extinction map of Perseus shows a chain of dark clouds. All of the known dark clouds and star-forming regions are seen with highest extinction.

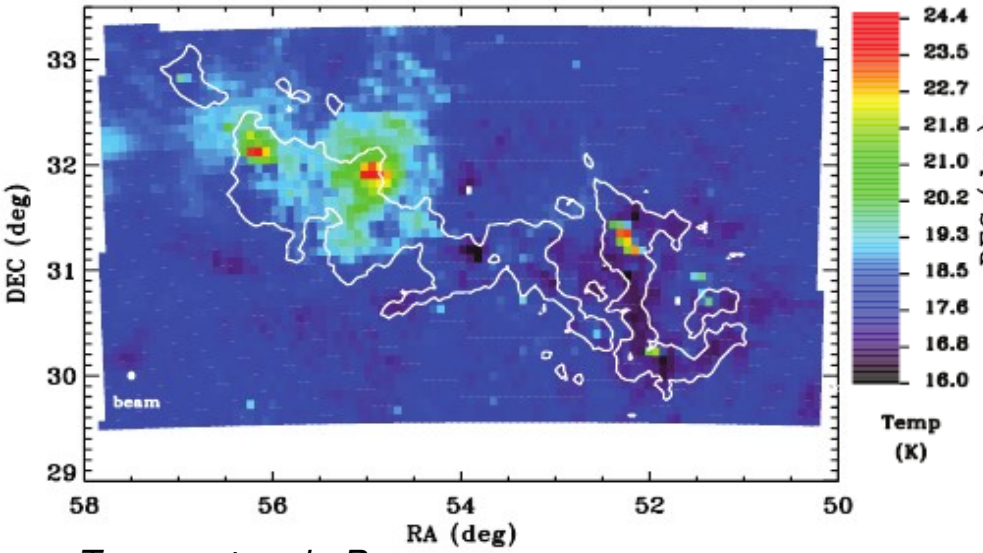

Temperature in Perseus. *(Ridge et al. 2006)*

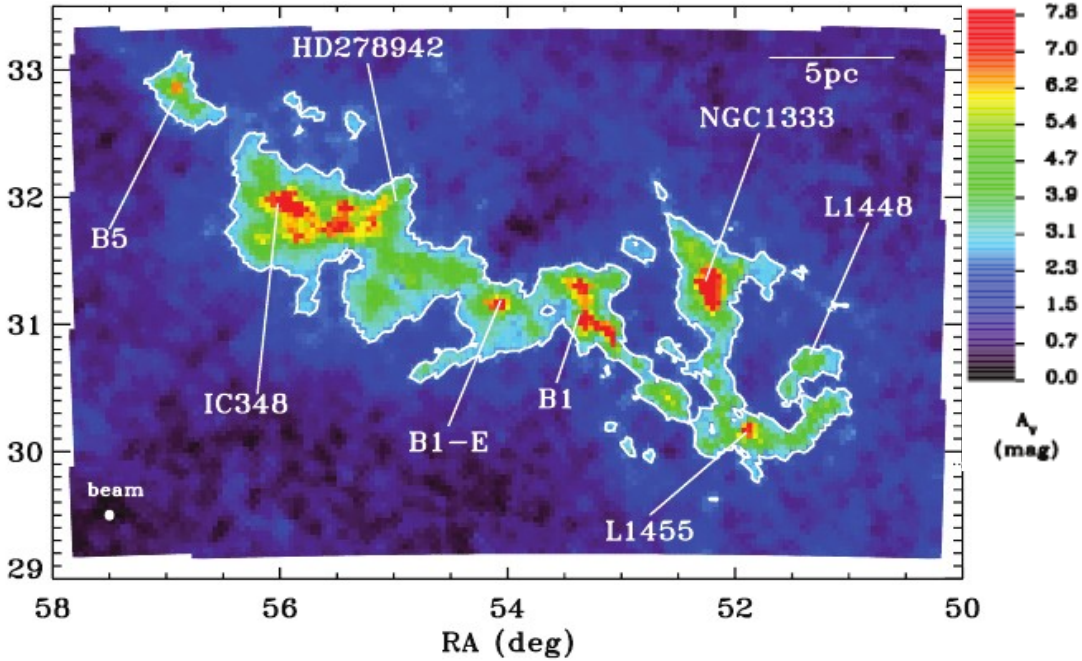

Map of extinction in Perseus. *(Ridge et al. 2006)*

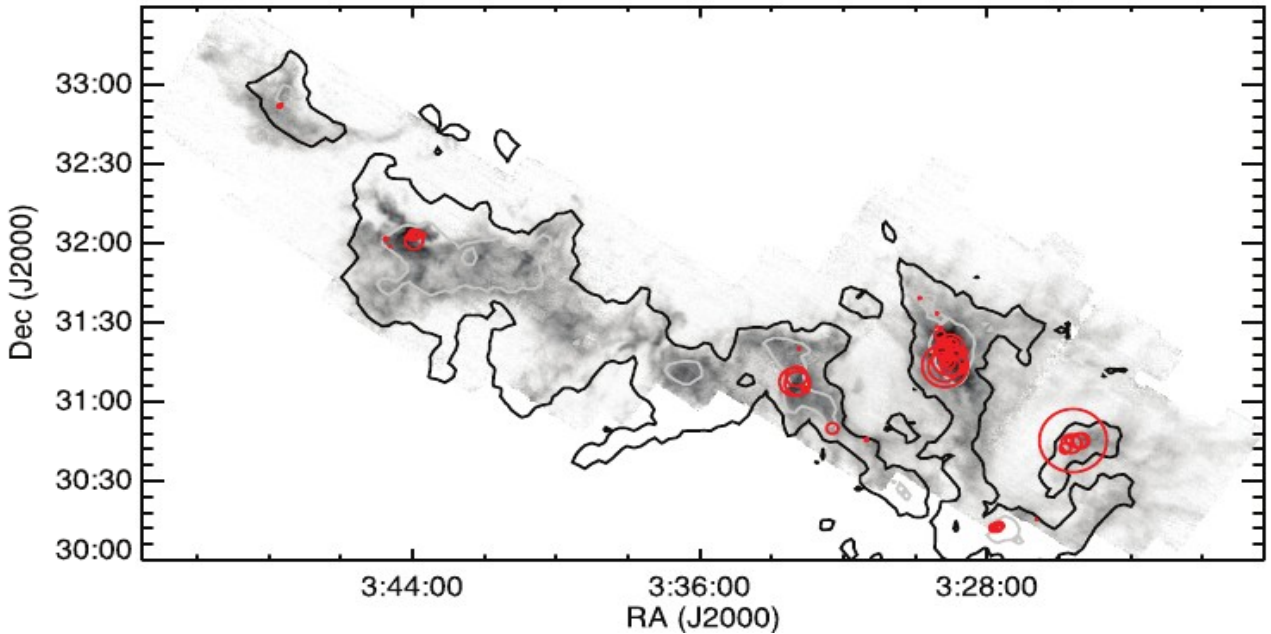

The morphology of the integrated CO intensity in Perseus is similar to that of the extinction, but reveal complex substructure within the clumps seen in extinction.

^{13}CO emission in Perseus, overlaid with the positions of the dense cores detected in submm continuum emission (red circles). Symbol size is proportional to the mass of the core. *(Ridge et al. 2006)*

PROTOSTELLAR ENVELOPES: Class 0 source Barnard 1c (B1-c) in Perseus

Barnard 1c is a potential star-forming in the main molecular core of Barnard 1 in the Perseus cloud complex.

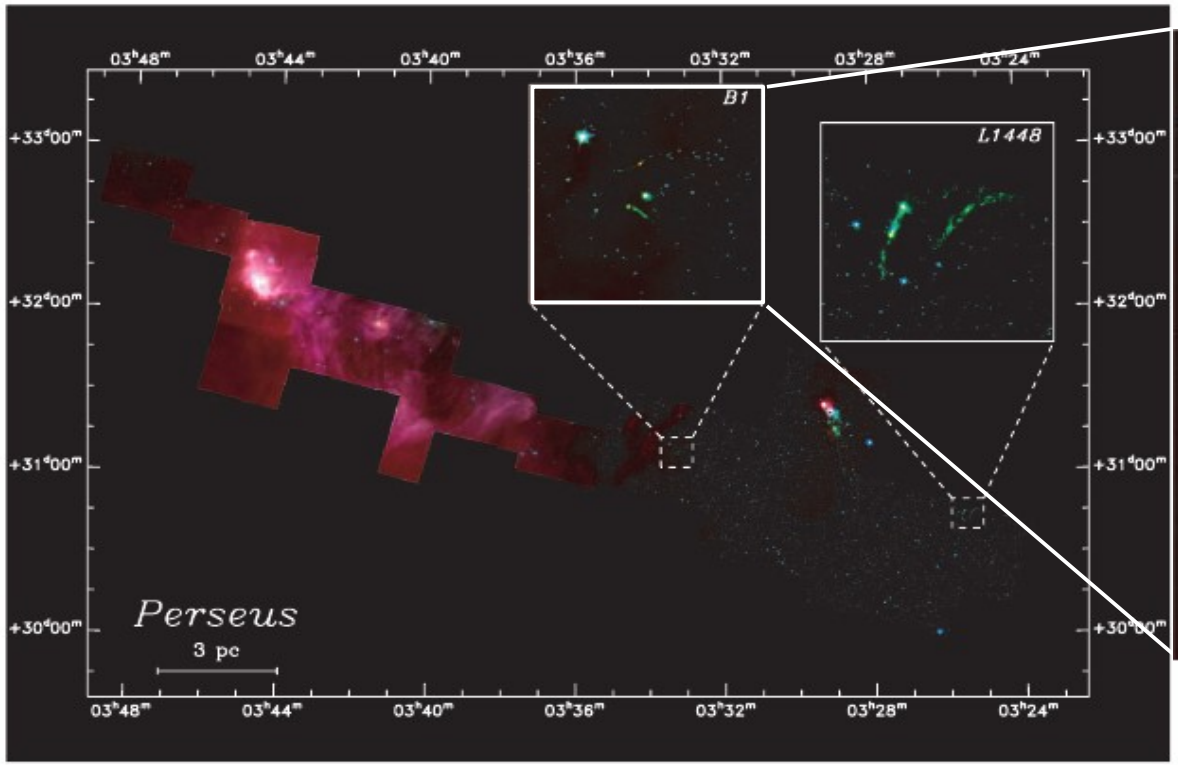

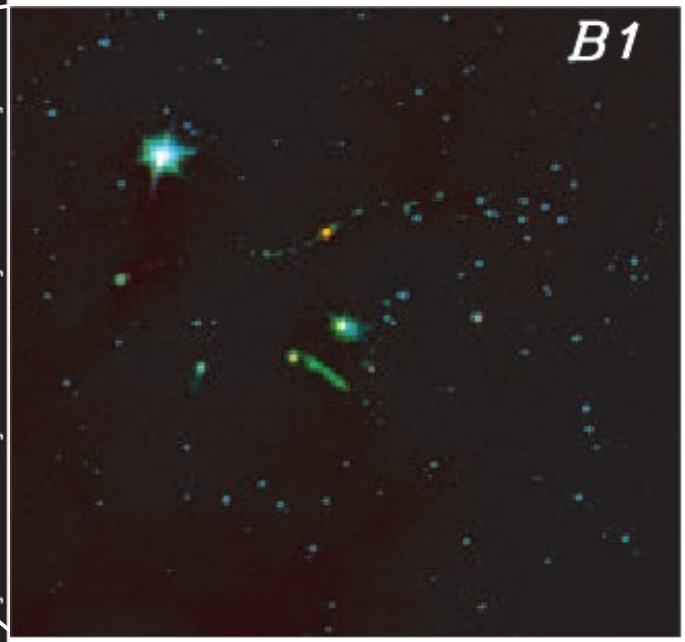

Three-color image of the Perseus region with 3.6 μm (blue), 4.5 μm (green), and 8.0 μm (red). (Jørgensen et al. 2006)

The SED resembles a blackbody with T ≤ 30 K. At this stage, the protostar and its disk are obscured by the infalling envelope.

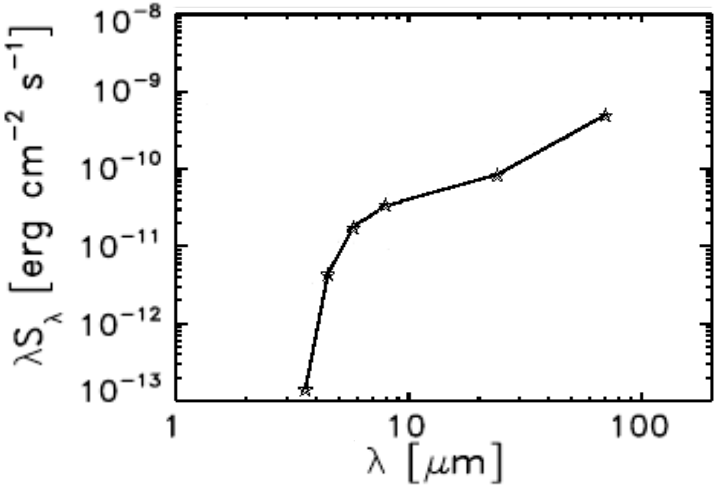

SED of the B1-c class 0 object. (original figure from Jørgensen et al. 2006)

PROTOSTELLAR ENVELOPES: Class 0 source Barnard 1c (B1-c) in Perseus

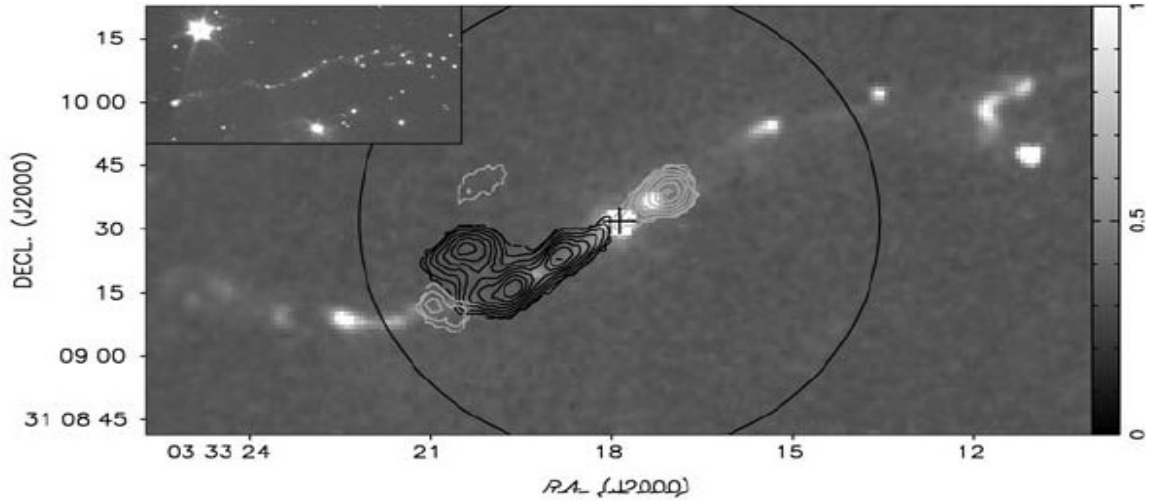

CO 1–0 emission over a 4.5 μm image (greyscale). (Jørgensen et al. 2006) The cross marks the position of the 3 mm continuum peak. (Matthews et al. 2008)

The most strongly red-shifted (gray contours) and blue-shifted (black contours) emission lies close to the protostar.

The material at the leading edge of the blue-shifted lobe appears red-shifted relative to the velocity of the source.

Schematic of the morphology of B1-c: The centrally heated cavity and outflow cavity are indicated by absence of N_2H^+. *(Matthews et al. 2008)*

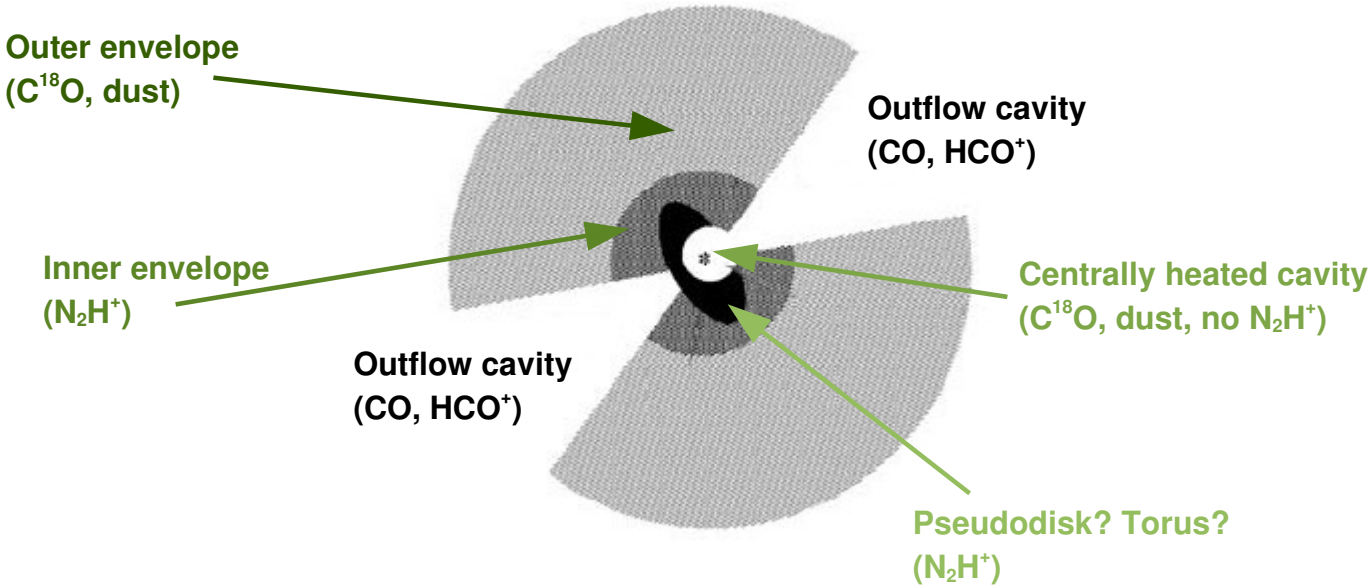

PROTOSTELLAR ENVELOPES: Class 0 source Barnard 1c (B1-c) in Perseus

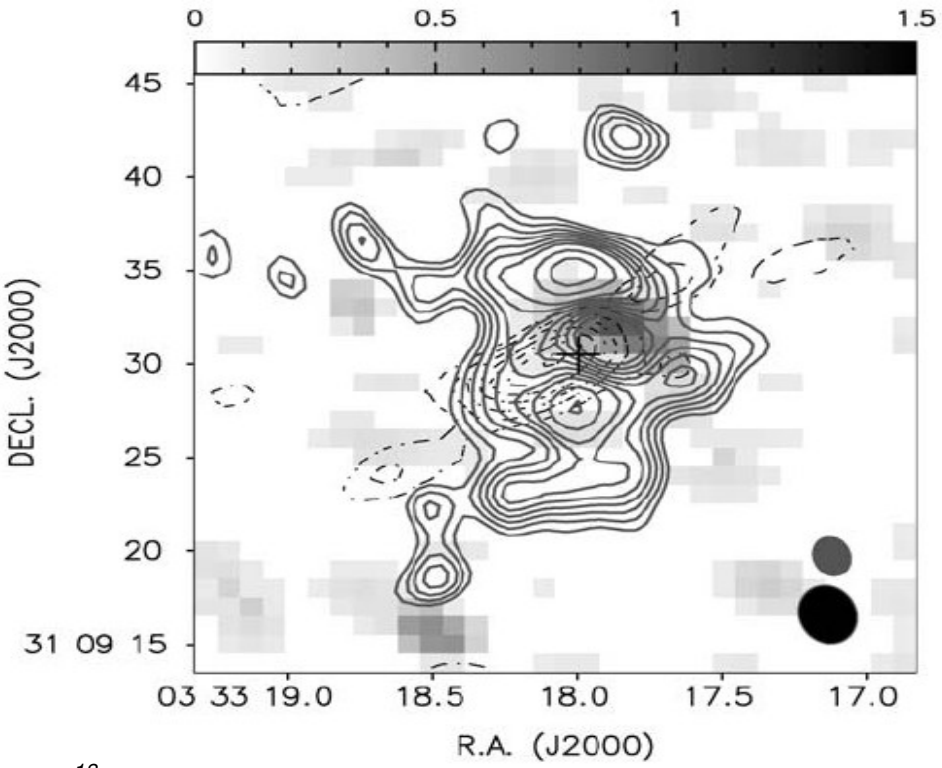

$C^{18}O$ 2 – 1 emission (grayscale) and N_2H^+ (contours). (Matthews et al. 2008)

A central cavity can be identified in N_2H^+ emission. Its anticorrelation with $C^{18}O$ emission suggests that heating in the center has released CO from grain mantles, in turn destroying N_2H^+.

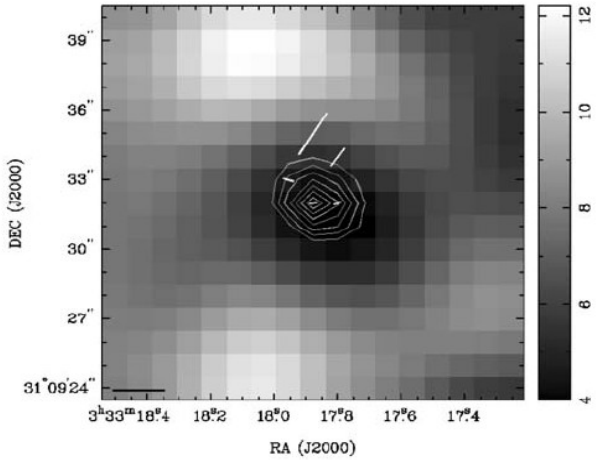

N_2H^+ emission of B1-c (grayscale; white indicates high emission, black indicates diminished N_2H^+ emission) on a 850 μm continuum image (gray contours). Length of the vectors indicates polarization percentage. (Matthews et al. 2008)

The declining emissivity of grains and the lower fluxes of dust emission at longer wavelengths makes 850 μm measurements superior to 1.3 mm observations.

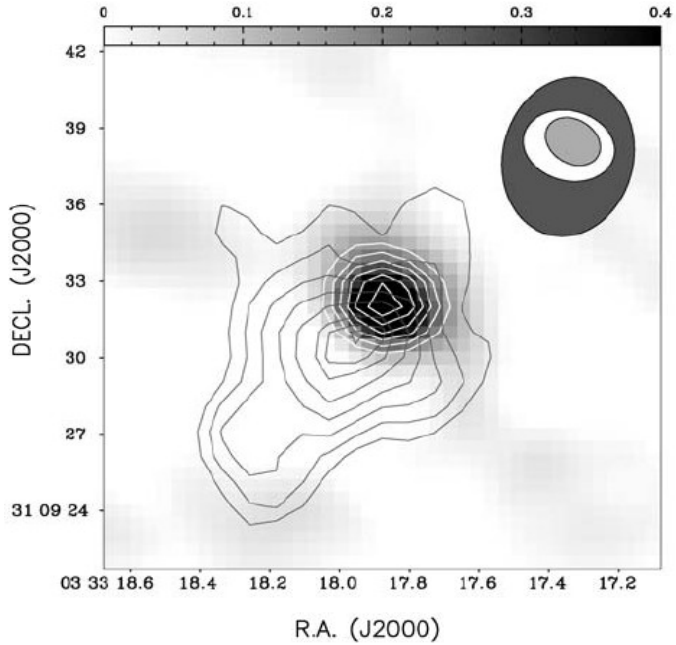

Continuum emission at 3 mm (gray contours), 1 mm (white contours) and 850 μm (grayscale). (Matthews et al. 2008)

As the envelope's material continues to infall onto the disk, it eventually becomes thin and transparent and the YSO becomes observable (far-IR, visible).
The protostar begins to fuse deuterium and then ordinary hydrogen.
The external appearance of the YSO at this stage corresponds to the spectral class I protostars (YTTS).
The forming star has already accreted much of its mass (80-90% of the system).

PROTOSTELLAR ENVELOPES: Class I source Butterfly Star in Taurus

(IRAS 04302 + 2247)

- later stage of protostellar collapse
- displays very broad SEDs that peak near 100 μm
- envelope masses are similar to the mass of the central pre-main-sequence core
- well-developed accretion disks
- envelopes have bipolar cavities excavated by outflows

PROTOSTELLAR ENVELOPES: Class I Butterfly Star in Taurus

The Butterfly star is a class I protostar in the Taurus-Auriga molecular cloud complex whose equatorial plane is inclined edge-on to the LOS (incl. ~90°).

The near-IR appearance is dominated by the totally opaque band extending 900 AU north/south that bisects the scattered light nebulosity.

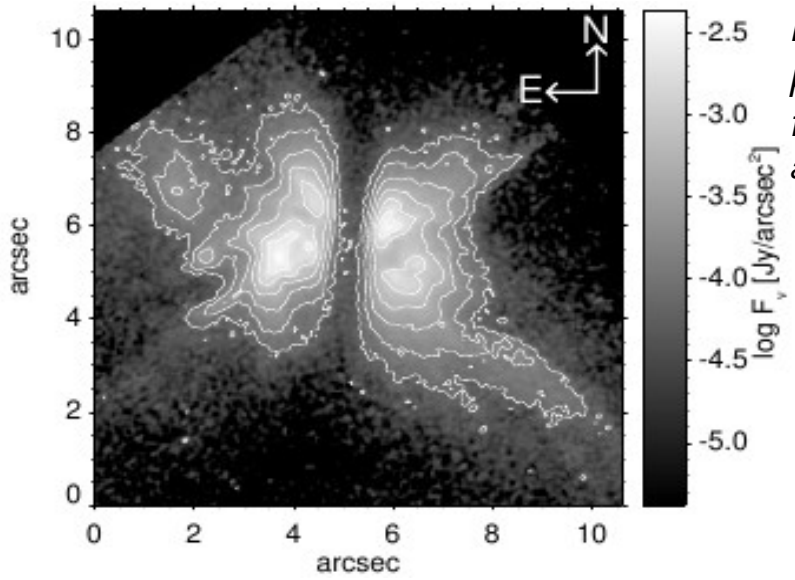

HST 1.6 μm surface photometry. Contours double in flux with each level. *(Padgett et al. 1999)*

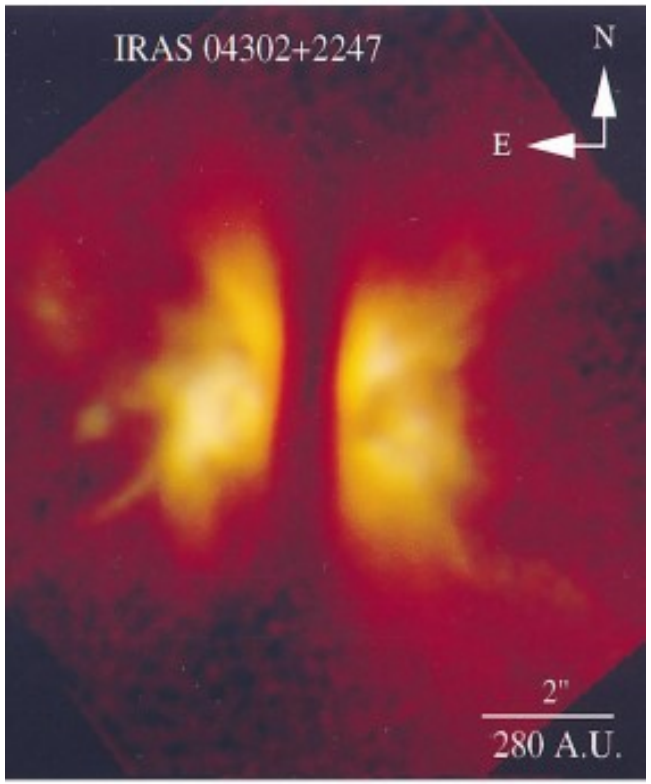

HST pseudo-true color composite image of 1.1 μm, 1.6 μm, and 2.05 μm observations. *(Padgett et al. 1999)*

The dark lane coincides with a dense rotating disk of molecular gas and may therefore be a large optically thick circumstellar disk seen precisely edge-on.

PROTOSTELLAR ENVELOPES: Class I Butterfly Star in Taurus

Mm-mapping of this source in ^{13}CO 1-0 indicates that the dark lane coincides with a dense rotating disk of molecular gas.

The dust lane may therefore be a large optically thick circumstellar disk seen precisely edge-on.

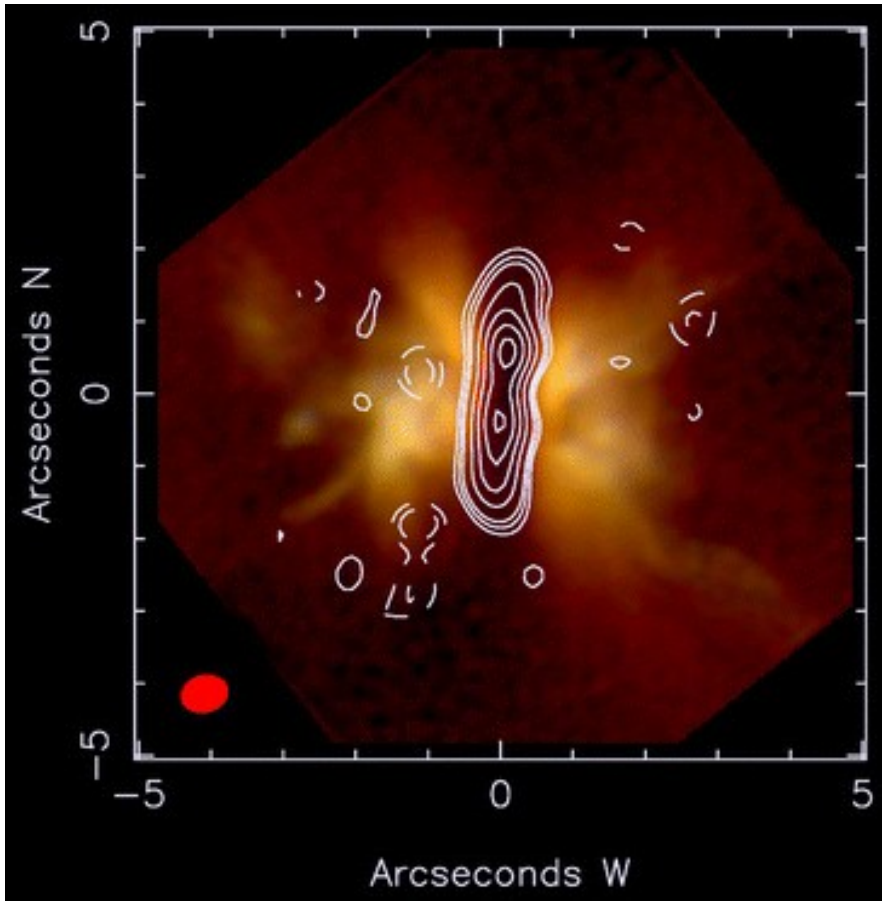

Sub-mm map of the Butterfly star (894 μm, contour lines), overlaid on the near-IR scattered-light map. (Wolf et al. 2003b; Padgett et al. 1999)

Near-IR and mm wavelength images show that the grains in the envelope of this object cannot be distinguished from those of the ISM and that the grains the much denser circumstellar disk have grown via coagulation by up to 2–3 orders of magnitude.

The separated dust grain evolution is in agreement with the theoretical prediction of a sensitive dependence of grain growth on the location in the circumstellar environment of young (proto)stars:

Grain growth is expected to occur on much shorter timescales in the dense region of circumstellar disks than in the thin circumstellar envelope. For the same reason a radial dependence of the dust grain evolution in the disk itself is expected. *(Wolf et al. 2003b)*

PROTOSTELLAR ENVELOPES: Class I Butterfly Star in Taurus

The system is assumed to consist of a circumstellar disk and an infalling envelope.

The circumstellar disk is assumed to be responsible for both the dark lane in the optical/IR wavelength range and the mm structure of the object. An additional envelope is required to explain the extended scattered light structure.

Although an infalling envelope, seen perpendicular to their axis of rotation symmetry, may also create a dark lane that hides the central star at optical and IR wavelengths, the observed sharp transition of the dark lane toward the scattered light regions, points to the presence of a disk. *(Wolf et al. 2003a)*

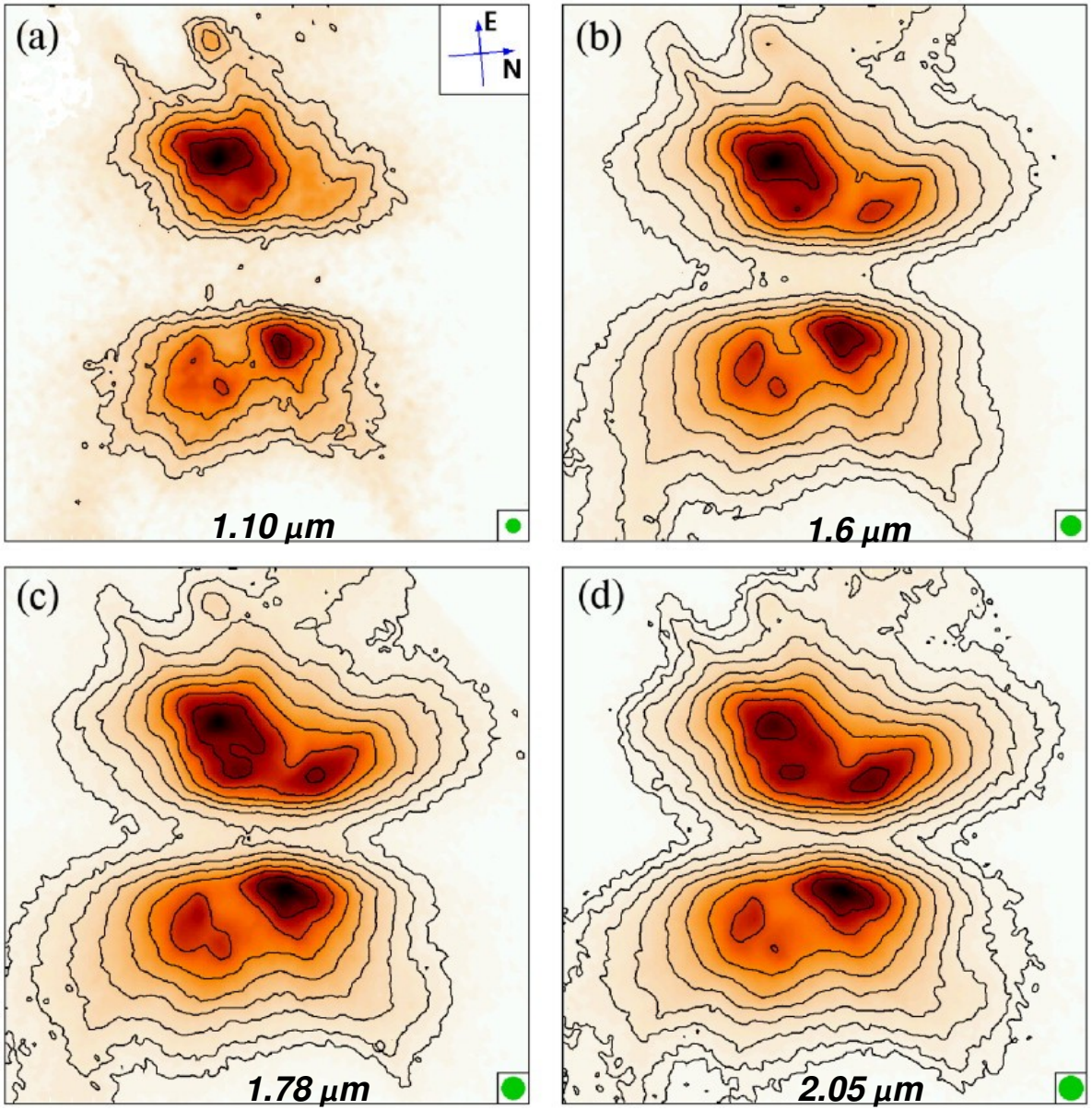

HST near-IR images. Assuming a distance of 140 pc, the side length of the images is 900 AU. Contours mark steps of 0.5^{m}. (Wolf et al. 2003a)

PROTOSTELLAR ENVELOPES: Class I Butterfly Star in Taurus

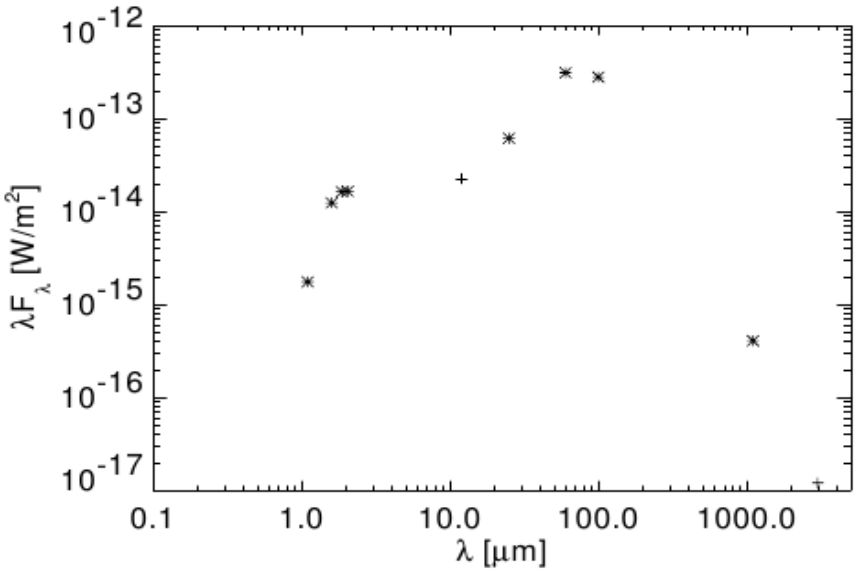

The IR SED is broad and peaks around 100 μm. The large IR excess arises from the well-developed accretion disk at this stage of the evoluion.

In the wavelength interval 10 μm – 3 mm most of the dust reemission occurs.

(Padgett et al. 1999)

The result of simulations shows a very good agreement with the observed SED in case of assuming an envelope+disk system, with the envelope being extended to a maximum distance of 450 AU from the star.

Comparing the dust reemission SED of the disk alone with the reemission of the whole system (disk +envelope), one finds that the SED is dominated by the reemission from the envelope up to a wavelength of about 174 μm. *(Wolf et al. 2003)*

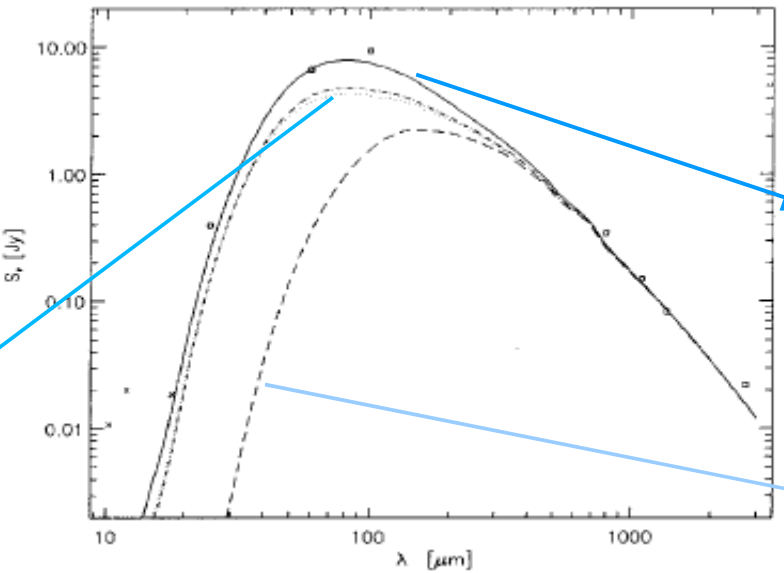

Envelope+disk model with an extended envelope

Envelope+disk model

Pure disk reemission (no envelope) model

As the envelope completely disappears, the protostar becomes a classical T Tauri star.
The mass of the disk around a classical T Tauri star is about 1–3% of the stellar mass.
A pair of bipolar jets is usually present as well.
Strong emission lines form as the accreted gas hits the "surface" of the star, which happens around its magnetic poles.

PROTOSTELLAR ENVELOPES: Class II source HV Tau C

- characterized by the presence of excess infrared emission above that expected for a stellar photosphere
- SED emission peak occurring in the near-IR
- dispersal of the remnant infall envelope by the combined effects of infall and outflow

PROTOSTELLAR ENVELOPES: Class II source HV Tau C

HV Tau A, HV Tau B, and HV Tau C were revealed to be a triple system with an edge-on disk inclined by 85° around HV Tau C.

They are located in the Taurus molecular cloud (140 pc) and are two of the brightest young stellar object with edge-on disks.

HV Tau C has 10 μm flux excess relative to the estimated spectrum of the central star, while HV Tau A, HV Tau B shows no infrared excess.

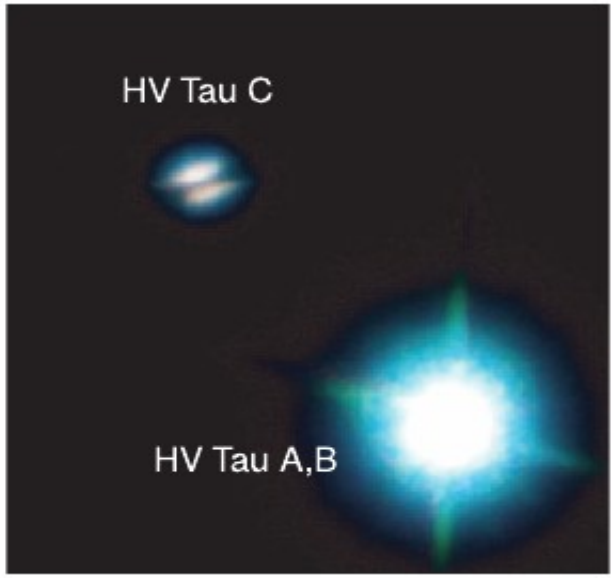

1.63 μm, 2,19 μm, and 3.72 μm color-composite image in log-scale for the HV Tau system. The field of view is 6.77" squared. (Terada et al. 2007)

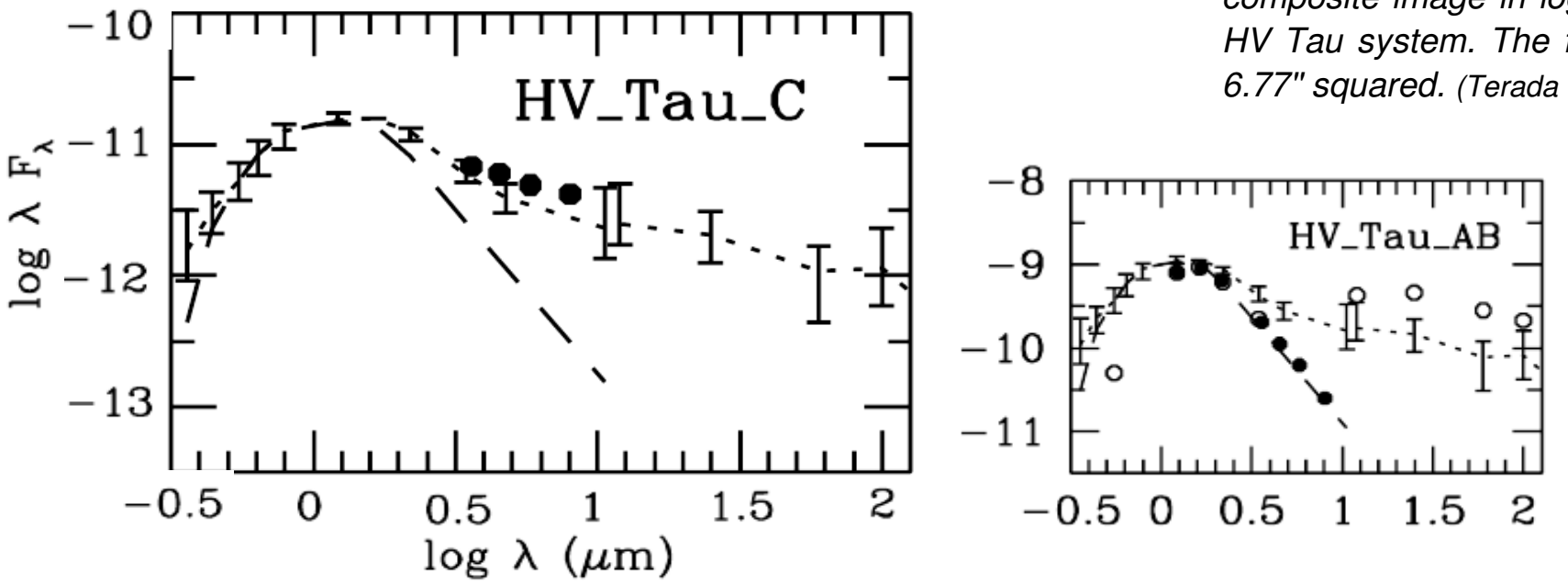

SEDs of HV Tau C and the HV Tau AB binary system. IRAC fluxes are combined with data from 2MASS (filled circles) and with ground-based and IRAS data (open circles). The (dereddened) SED of a class III (dashed line) and the median SED of a class II object (dotted line with error bars) is shown. (Hartmann et al. 2005)

PROTOSTELLAR ENVELOPES: Class II source HV Tau C

HV Tau C exhibits scattered light in an edge-on disk, and its two components are clearly resolved in all the bands.

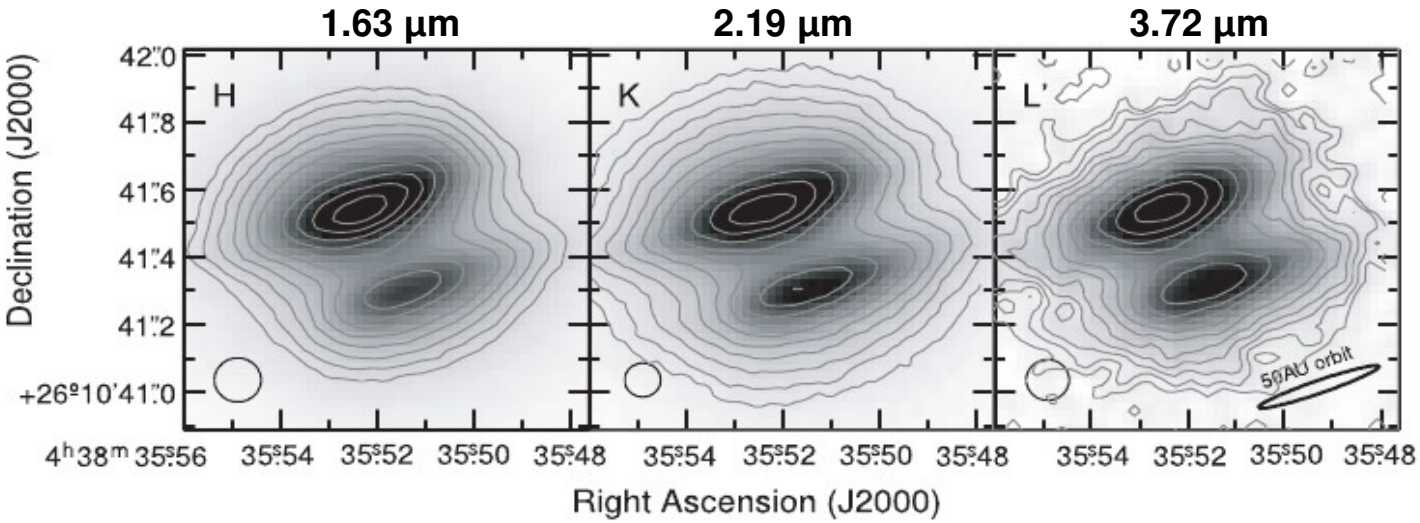

Surface brightness map of HV Tau C. A 50 AU circular orbit with an inclination angle of 84 °. (Terada et al. 2007)

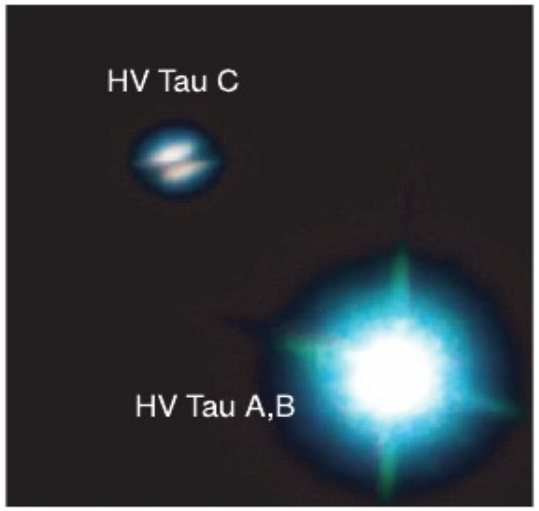

1.63 µm, 2,19 µm, and 3.72 µm color-composite image in log-scale for the HV Tau system. (Terada et al. 2007)

The width of the dark lane of HV Tau C is estimated by the distance between the peak of the two components of the scattered light from HV Tau C. The width is wider at the shorter wavelengths as expected by the greater extinction at the shorter wavelengths. *(Terada et al. 2007)*

On each side, bright lobes correspond to photons from the central star scattered back to the observer in the disk's upper layers and in optically thin bipolar cavities. The central star itself is not seen, being heavily extincted by the disk midplane. *(Monin and Bouvier 2000)*

PROTOSTELLAR ENVELOPES: Class II source HV Tau C

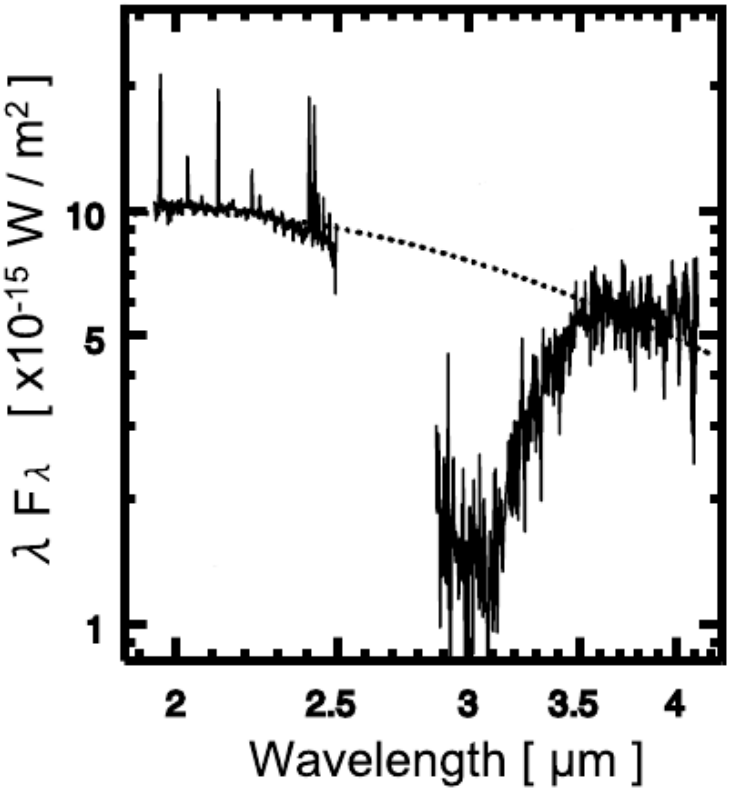

The spectra show a deep water ice absorption at 3 μm. In addition, many emission and absorption lines can be seen.

Since HV Tau C is well known to have a strong outflow activity, the most prominent emission lines are due to molecular hydrogen lines excited by the jet.

1.93–4.13 μm spectra of HV Tau C on 18 Jan. 2005. The dotted line indicates the continuum of the spectrum. (Terada et al. 2007)

The scattered light from the central star originates within a radius 50 AU from HV Tau C. Thus, it is likely that the material responsible for the ice absorption is outside the scattered light region. *(Stapelfeldt et al. 1998, 2003)*

Since the midplane disk is optically thick in the 3 μm band, we can observe only the scattered light through the regions above and below the midplane disk.

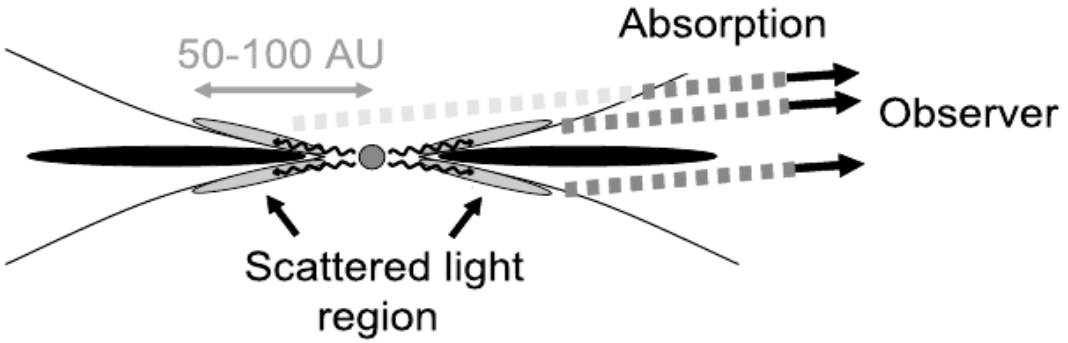

Schematic view of geometry for the water ice absorption. Gray elliptical areas: scattered light regions; black elliptical areas: midplane of the flared disk. (Terada et al. 2007)

The disk eventually disappears due to accretion onto central star, planet formation, ejection by jets and photoevaporation by UV-radiation from the central star and nearby stars.
As a result the young star becomes a weakly lined T Tauri star, which slowly which evolves into an ordinary sun-like star.

PROTOSTELLAR ENVELOPES: Class III source DoAr 25

- SEDs that resemble a stellar photosphere
- not known for certain whether Class III sources are more evolved than the Class II sources or whether they have simply lost most of their circumstellar material on a faster timescale
- stage ends in a zero-age main-sequence star

PROTOSTELLAR ENVELOPES: Class III source DoAr 25

DoAr 25 is located in the L1688 dark cloud in Ophiuchus.

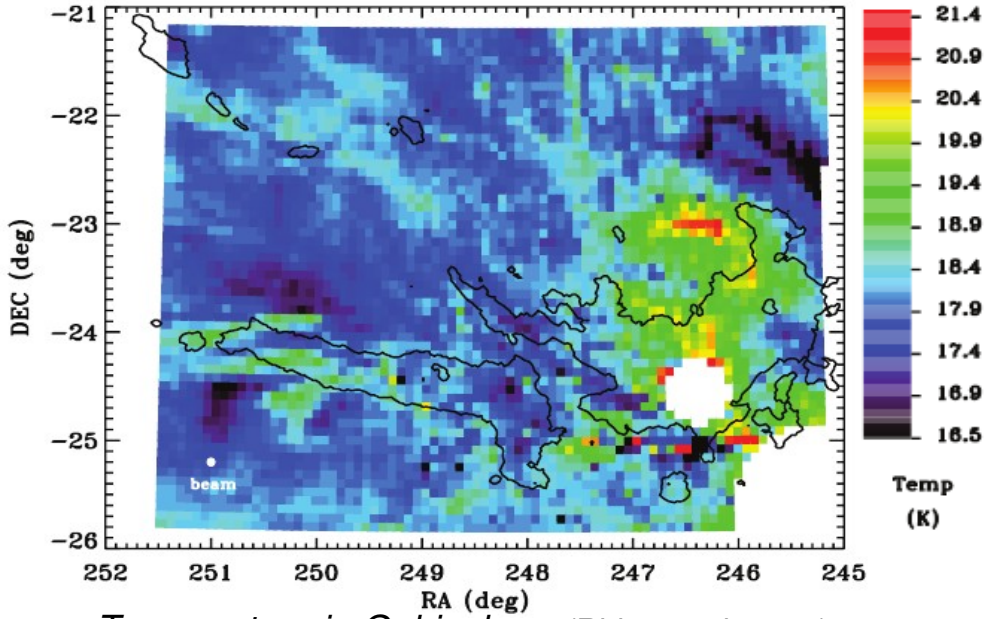

Temperature in Ophiuchus. *(Ridge et al. 2006)*

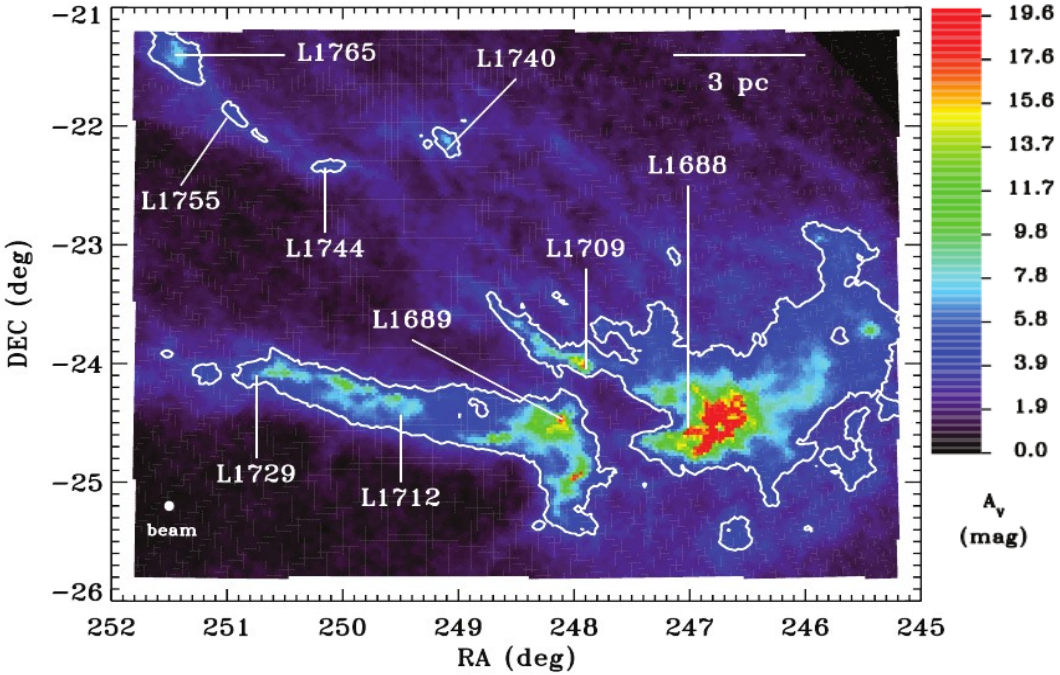

Map of extinction in Ophiuchus. *(Ridge et al. 2006)*

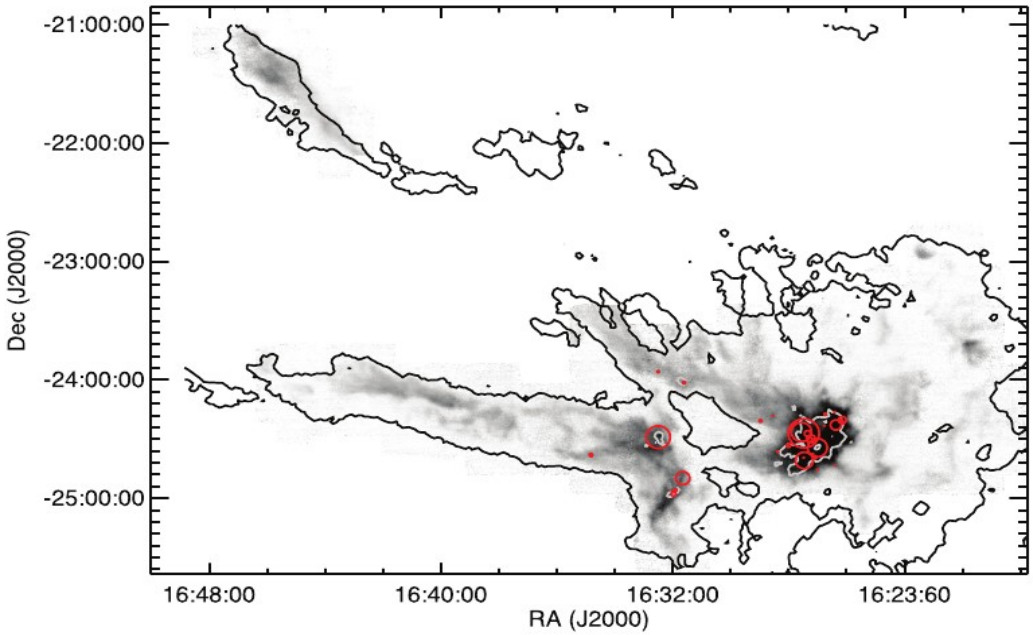

The map of Ophiuchus reveals a multi-filamentary structure with the very opaque L1688 dark cloud showing highest extinction.

^{13}CO emission in Ophiuchus, overlaid with the positions of the dense cores detected in submm continuum emission (red circles). Symbol size is proportional to the mass of the core. *(Ridge et al. 2006)*

PROTOSTELLAR ENVELOPES: Class III source DoAr 25

The high spatial resolution 865 μm continuum image indicates a well-resolved source with an inclination of about 62°. *(Andrews et al. 2008)*

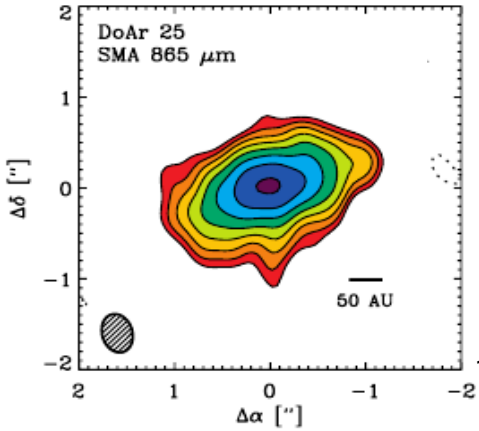

High-resolution image of the 865 μm continuum emission. Contours increase by factors of √2. (Andrews et al. 2008)

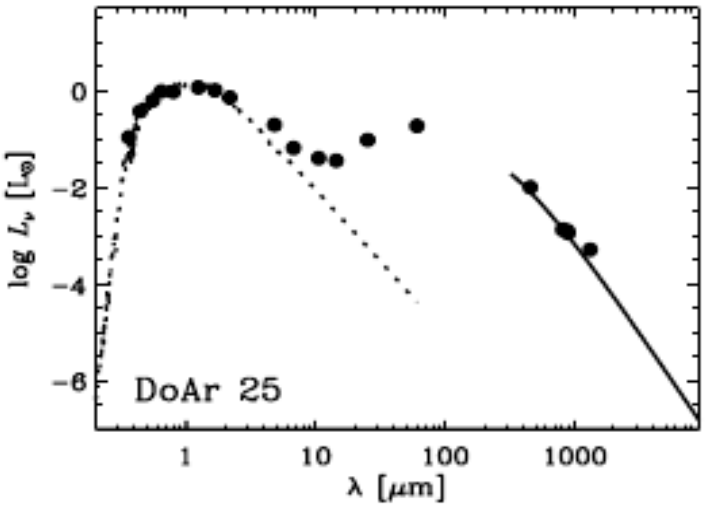

The IR SED shows a relatively small thermal excess above the stellar photosphere out to mid-IR wavelengths.

Pronounced dips in the IR SED suggest that large inner holes or gaps have been cleared. *(Andrews & Williams 2007)*

Despite its bright mm emission, this source exhibits only a comparatively small IR excess, suggesting that the material and structural properties of the inner disk may be in an advanced state of evolution. *(Andrews et al. 2008)*

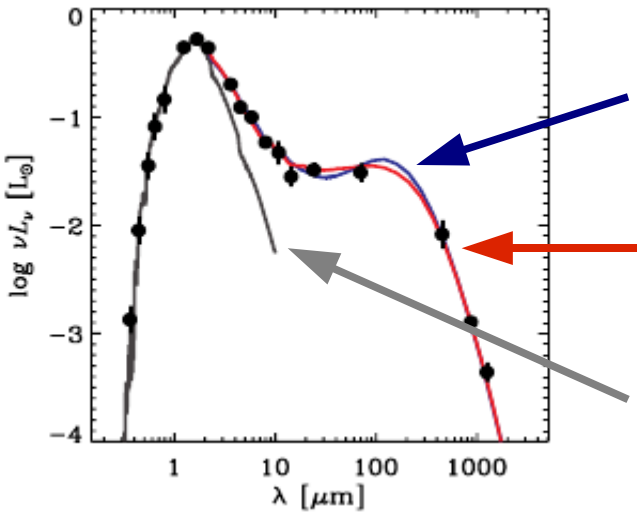

Distribution with grain growth (and reduced emissivity) in the inner disk (r < 40 AU)

SED of a model disk for a standard grain size distribution

Input stellar radiation source for the radiative transfer modeling

PROTOSTELLAR ENVELOPES: Summary

Stars form from collapsing clouds of gas and dust and in their earliest infancies are surrounded by complex environments that obscure our view at optical wavelengths.

As evolution proceeds, a stage is revealed with three main components:

- *the young star*
- *a circumstellar disk*
- *an infalling envelope*

Most disks around young low- and intermediate-mass stars fall into one of two categories: *(Watson et al. 2007)*

YSO disks (characterized by dust growth):

- optically thick at visible and near-IR wavelengths
- rich in molecular gas
- found around Class I and Class II systems

Debris disks (characterized by planetesimal destruction):

- optically thin at optical and near-IR wavelengths
- only trace quantities of gas
- found around Class III and older systems

PROTOSTELLAR ENVELOPES: Summary

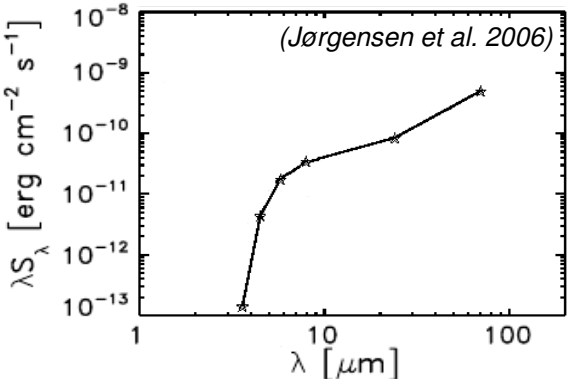

- *Star plus nebular disk formation*
- *Most material falls onto the disk*
- *An accretion-driven stellar or disk wind begins to clear envelope gas away from the rotational poles*
- *Object in this early embedded YSO phase are completely invisible at λ < 25 μm*

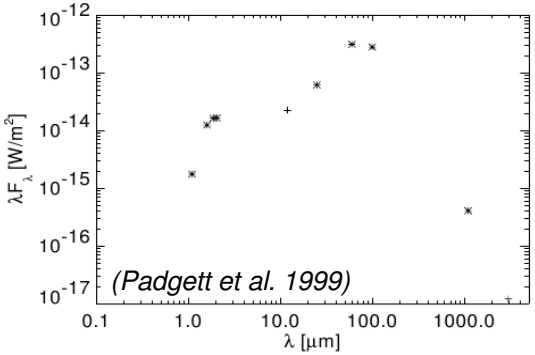

- *The later "embedded YSO phase" (YTTS)*
- *Spectrum rises beyond 2 μm*
- *In most embedded objects, most the scattered light from walls of the outflow cavity in the envelope*
- *The embedded phase is thought to last for a few times 10^5 yr*

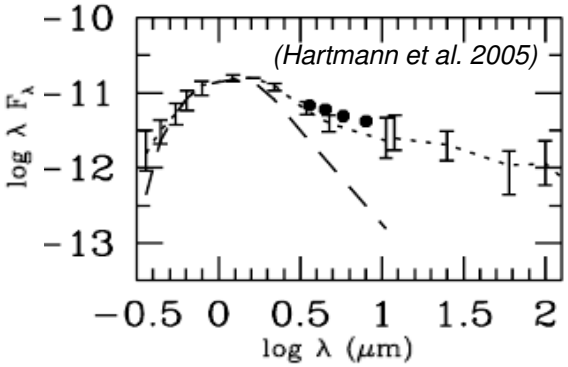

- *The infalling envelope disperses*
- *Optically visible "classical" T Tauri star (CTTS) with a circumstellar disk*
- *Accretion through the disk slows, but continues*
- *This "Class II" phase lasts from 10^6-10^7 yr*
- *Spectrum has near-IR to far-IR excess of photospheric values, but flat or falling longward of 2 μm*
- *Light reflected from the top and/or bottom surfaces of an optically thick disk will dominate*

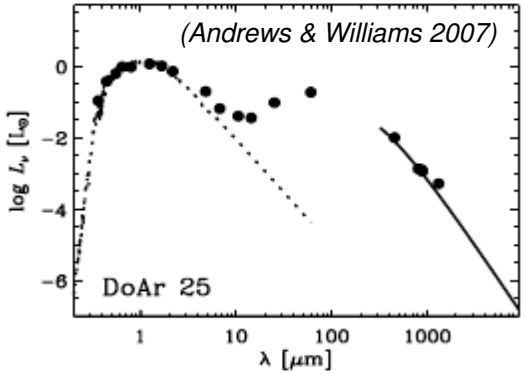

- *Accretion through the disk subsides due to lack of replenishment or disk gaps*
- *The disk becomes optically thin, and the system evolves into a "weak-lined" T Tauri star (WTTS)*
- *Spectrum is that of a stellar photosphere with a small amount of infrared excess at mid-IR and far-IR*
- *No emission lines as strong as those of the CTTS*

PROTOSTELLAR ENVELOPES: References

- P. W. Lucas and P. F. Roche, ***Further observations of IRAS 04302+2247***, Mon. Not. R. Astron. Soc. 299, 723–727 (1998)

- D. L. Padgett, W. Brandner, K. R. Stapelfeldt, S. E. Strom, S. Terebey, and David Koerner, ***HUBBLE Space Telescope/NICMOS imaging of disks and envelopes around very young stars***, The Astrophysical Journal,, 117, 1490-1504, (1999)

- J.-L. Monin, and J. Bouvier, ***Disks in multiple systems: direct imaging of a nearly edge-on circumstellar disk in the young triple system HV Tau***, Astron. Astrophys. 356, L75–L78 (2000)

- M. Simon, A. Dutrey, and S. Guilloteau, ***Dynamical masses of T Tauri stars and calibration of pre-main-sequence evolution***, The Astrophysical Journal, 545, 1034-1043, (2001)

- B. C. Matthews and C. D. Wilson, ***Magnetic fields in star-forming molecular clouds. V. Submillimeter polarization of the Barnard 1 dark cloud***, The Astrophysical Journal, 574, 822–833, (2002)

- S. Wolf, D. L. Padgett, and K. R. Stapelfeldt, ***The circumstellar disk of the Butterfly star in Taurus***, The Astrophysical Journal, 588, 373–386, (2003)

- L. Hartmann, S. T. Megeath, L. Allen, K. Luhman, N. Calvet, P. D'Alessio, R. Franco-Hernandez, and G. Fazio, ***IRAC observations of Taurus pre-main-sequence stars***, The Astrophysical Journal, 629, 881–896, (2005)

- J. K. Jørgensen, P. M. Harvey, N. J. Evans II, T. L. Huard, L. E. Allen, A. Porras, G. A. Blake, T. L. Bourke, N. Chapman, L. Cieza, D. W. Koerner, S.-P. Lai, L. G. Mundy, P. C. Myers, D. L. Padgett, L. Rebull, A. I. Sargent, W. Spiesman, K. R. Stapelfeldt, E. F. van Dishoeck, Z. Wahhaj, and K. E. Young, ***The SPITZER C2D survey of large, nearby, interstellar clouds. III. Perseus observed with IRAC***, The Astrophysical Journal, 645, 1246–1263, (2006)

- N. A. Ridge, J. Di Francesco, H. Kirk, D. Li, A. A. Goodman, J. F. Alves, H. G. Arce, M. A. Borkin, P. Caselli, J. B. Foster, M. H. Heyer, D. Johnstone, D. A. Kosslyn, M. Lombardi, J. E. Pineda, S. L. Schnee, and M. Tafalla, ***The complete survey of star-forming regions: Phase I data***, The Astronomical Journal, 131, 2921–2933, (2006)

- S. M. Andrews and J. P. Williams, ***High-resolution submillimeter constraints on circumstellar disk structure***, The Astrophysical Journal, 667:303–307, (2007)

- H. Terada, A. T. Tokunaga, N. Kobayashi, N. Takato, Y. Hayano, and H. Takami, ***Detection of water ice in edge-on protoplanetary disks: HK Tauri B and HV Tauri C***, The Astrophysical Journal, 659, 705-728, (2007)

- A. M. Watson, K. R. Stapelfeldt, K. Wood, and F. Ménard, ***Multi-Wavelength Imaging of Young Stellar Object Disks: Toward an Understanding of Disk Structure and Dust Evolution***, in ***Protostars and Planets V***, B. Reipurth, D. Jewitt, and K. Keil (eds.), (2007)

- S. M. Andrews, A. M. Hughes, D. J. Wilner, and C. Qi, ***The structure of the DoAr 25 circumstellar disk***, The Astrophysical Journal, 678: L133–L136, (2008)

- B. Matthews, E. Bergin, A. Crapsi, M. Hogerheijde, J. Jørgensen, D. Marrone, and R. Rao, ***The Class 0 source Barnard 1c. Most recent results***, Astrophys Space Sci, 313, 65–68, (2008)

- S. Wolf, A. Schegerer, H. Beuther, D. L. Padgett, and K. R. Stapelfeldt, ***Submillimeter structure of the disk of the Butterfly star***, The Astrophysical Journal, 674, L101–L104, (2008)

PROTOSTELLAR ENVELOPES: Class 0 source Barnard 1c (B1-c) in Perseus

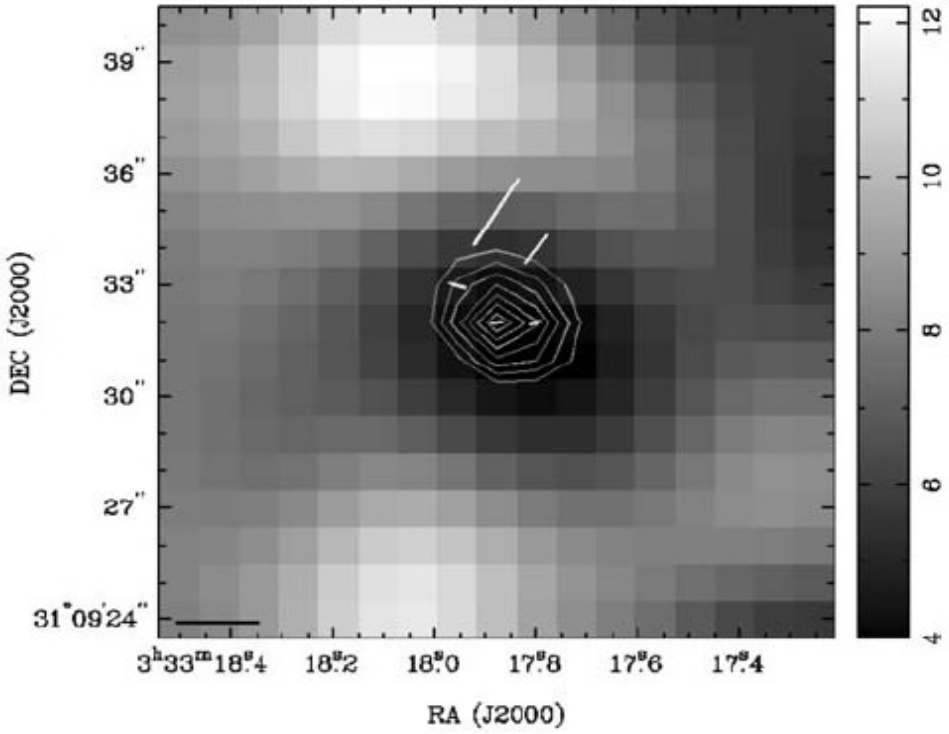

Grains without ice mantles are more effective at polarizing radiation in the diffuse interstellar medium. (*Whittet et al. 2001*)

Polarization within the heated cavity of B1-c. N_2H^+ (grayscale; white indicates high emission, black indicates diminished N_2H^+ emission) on a 850 μm continuum image (gray contours). Length of the vectors indicates polarization percentage. (*Matthews et al. 2008*)

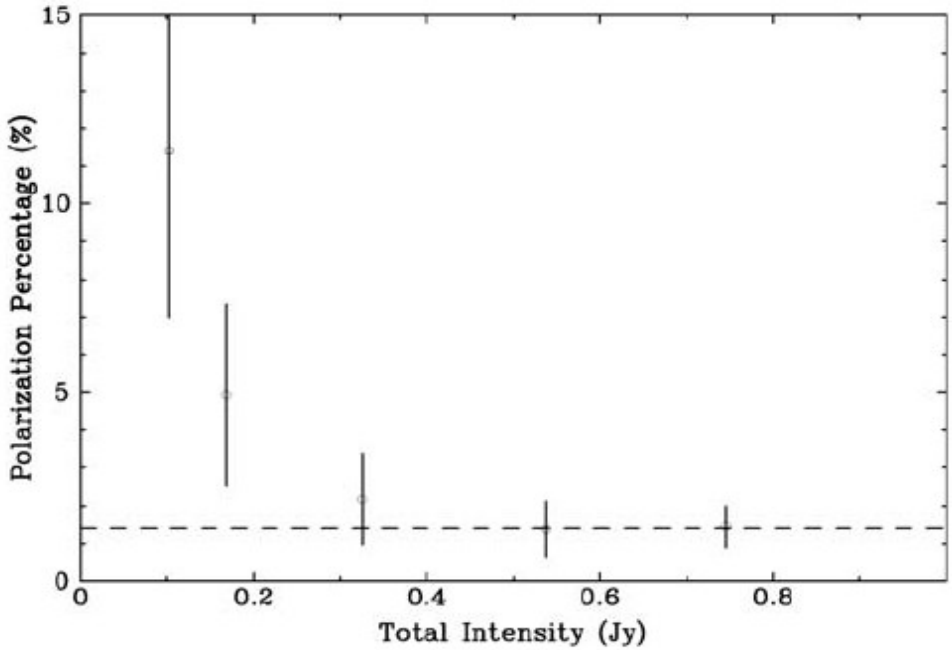

The uniform value of polarization percentage, and the anti-correlation of the N_2H^+ and $C^{18}O$ emission in the cavity indicate that all the grains are heated to a temperature sufficient to desorb CO from grain surfaces.

Polarization percentage as a function of measured intensity. Dashed line indicates 1.4% polarization. (*Matthews et al. 2008*)

PROTOSTELLAR ENVELOPES: Class 0 source Barnard 1c (B1-c) in Perseus

Maps of three Stokes parameters (I, Q, and U) are combined to yield the polarization percentage and polarization position angle according to the following relations:

$$p = \frac{\sqrt{Q^2 + U^2}}{I}, \quad \theta = \frac{1}{2}\arctan\left(\frac{U}{Q}\right) .$$

The uncertainties in each of these quantities are given by

$$dp = p^{-1}\sqrt{dQ^2Q^2 + dU^2U^2}, \quad d\theta = \frac{28.^{\circ}6}{\sigma_p} ,$$

where p is the signal-to-noise ratio in p, or p/dp.

The polarization percentages were debiased according to the expression

$$p_{\mathrm{db}} = \sqrt{p^2 - dp^2} .$$

B1-c was identified as a potential star-forming core in dust emission polarimetry measurements of the main molecular core of Barnard 1.

The core shows strong polarization, with evidence that the polarization percentage is constant to the core centre.

Typically, polarization percentage diminishes toward peaks in intensity, resulting in what are called ‘polarization holes’. *(Matthews and Wilson 2002)*

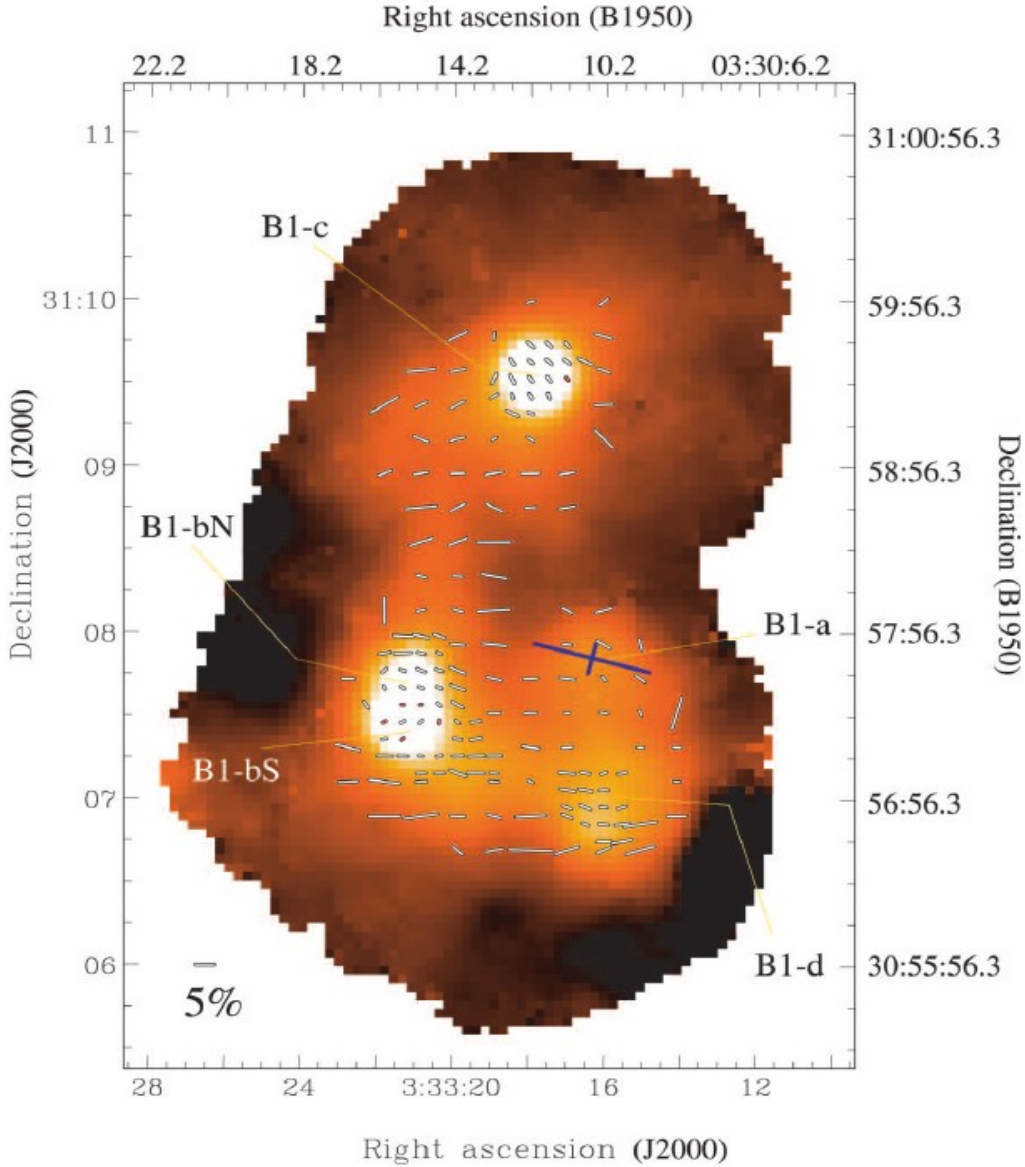

850 μm polarization pattern toward the main core of Barnard 1 overlaid on the Stokes I map. All vectors are associated with Stokes I values greater than 20% of the B1-d peak flux. Red vectors have polarization percentage, p, less than 1%. The vectors are accurate in position angle to better than 10°. (Matthews and Wilson 2002)